Au NASA 7N-05

191973

36P.

TECHNICAL NOTES

NATIONAL ADVISORY COMMITTEE FOR AERONAUTICS

No. 716

HYDRODYNAMIC AND AERODYNAMIC TESTS OF A FAMILY OF MODELS

OF SEAPLANE FLOATS WITH VARYING ANGLES OF DEAD RISE

N.A.C.A. MODELS 57-A, 57-B, AND 57-C

By John B. Parkinson, Roland E. Olson, and Rufus O. House
Langley Memorial Aeronautical Laboratory

Washington
July 1939

NATIONAL ADVISORY COMMITTEE FOR AERONAUTICS

TECHNICAL NOTE NO. 716

HYDRODYNAMIC AND AERODYNAMIC TESTS OF A FAMILY OF MODELS

OF SEAPLANE FLOATS WITH VARYING ANGLES OF DEAD RISE

N.A.C.A. MODELS 57-A, 57-B, AND 57-C

By John B. Parkinson, Roland E. Olson, and Rufus O. House

SUMMARY

Three models of V-bottom floats for twin-float sea-
planes (N.A.C.A. models 57-A, 57-B, and 57-C) having an-
gles of dead rise of 20°, 25°, and 30°, respectively, were
tested in the N.A.C.A. tank and in the N.A.C.A. 7- by 10-
foot wind tunnel. Within the range investigated, the ef-
fect of angle of dead rise on water resistance was found
to be negligible at speeds up to and including the hump
speed, and water resistance was found to increase with an-
gle of dead rise at planing speeds. The height of the
spray at the hump speed decreased with increase in angle
of dead rise and the aerodynamic drag increased with dead
rise.

Lengthening the forebody of model 57-B decreased the
water resistance and the spray at speeds below the hump
speed. Spray strips provided an effective means for the
control of spray with the straight V sections used in the
series but considerably increased the aerodynamic drag.

Charts for the determination of the water resistance
and the static properties of the model with 25° dead rise
and for the aerodynamic drag of all the models are includ-
ed for use in design.

INTRODUCTION

Seaplane floats are usually of the V-bottom type with
angles of dead rise of from 20° to 30°, angle of dead rise
being defined as the angle with the horizontal made by a
straight transverse line joining the keel with the chine.
The N.A.C.A. model-57 series of three float forms was de-
signed to investigate through this range the effect of

dead rise on water resistance, spray, and aerodynamic drag. The models of the series were tested in the N.A.C.A. tank and in the 7- by 10-foot wind tunnel at Langley Field, Va. The results of these tests are combined in this report in order that they may be useful in the design of twin-float seaplanes and in the conversion of landplanes for marine service.

DESCRIPTION OF MODELS

The lines of the models of the 57 series are shown in figure 1 and the offsets are given in tables I, II, and III. The length-beam ratio, the location of step, the angle of afterbody keel, and the depth of step are the same in each case and approximately conform to accepted practice for twin floats.

From station 6 aft, the sections below the chine are straight and have a constant angle of dead rise of 20°, 25°, and 30° for models 57-A, 57-B, and 57-C, respectively. Forward of station 6, the sections are arched to give finer water lines at the bow. From station 1/4 aft, the chines are fitted with spray strips, representing an outside juncture of side and bottom plating and providing a means of controlling spray. Above the chines the sections are rounded, the radius of the deck being equal to the half-breadth of the chine.

The plan form of the chine is the same for all the models. It is full forward and tapers aft to a square stern. The square stern provides more planing area aft and a more suitable form for attaching a water rudder with tiller bar than does a pointed stern although it has more drag in flight. For fairing, a tail similar to that of the Navy Mark V float (reference 1) could be added aft of the square stern with little effect on the water performance.

The height of the models was adjusted so that the maximum cross-sectional area and the total volume of the three forms are substantially the same. The profiles of the chines in the constant dead-rise portion are determined by the angle of dead rise and the half-breadth of the chine. Forward of station 6, the profiles of the chines are the same for all the models but are displaced vertically to suit the different heights at station 6. At each station forward of station 6, the height of the keel or a buttock

line above a horizontal plane through the keel at station 6 is the same proportion of the height of the chine above this plane for all three models.

· As a result of the method of derivation, the forms of the three models are very similar; the principal difference is the angle of dead rise over the planing bottom and the afterbody. The particulars of the family are:

Model	57-A	57-B	57-C
Angle of dead rise, deg.	20	25	30
Length, in.	84.00	84.00	84.00
Beam, in.	12.00	12.00	12.00
Beam over spray strips, in.	12.45	12.45	12.45
Depth, in.	11.09	11.40	11.73
Total volume, cu. in.	5,940	5,948	5,956
Maximum cross-sectional area, sq. in.	104.5	104.5	104.5

The wooden models are jointed at the step so that the angle of the afterbody and the depth of the step are adjustable. They were finished with gray pigmented varnish rubbed between coats. The spray strips were made of brass sheet and attached with wood screws at the chine, as shown in figure 1. The strips terminate at station 1/4, and it was assumed that the bow forward of this point will be in the form of a bumper pad.

During the tank tests, the bow of model 57-B was extended forward 10 inches by attaching a plywood skeleton to the bow and filling with beeswax. The resulting form, model 57-B-5, is shown dotted in figure 1 and the offsets for it are given in table IV. Photographs of the models showing the extended bow are shown in figure 2.

HYDRODYNAMIC TESTS

Apparatus and Procedure

The hydrodynamic tests were made in the N.A.C.A. tank (reference 2) using the towing gear described in reference 3. The models were tested free to trim at one condition of loading and at fixed trim by the general method over a wide range of loadings.

In the free-to-trim tests, the load on the water at each speed was adjusted by the hydrofoil lift device described in reference 3. The model was free to pivot about a position corresponding to an assumed center of gravity of a seaplane and it was balanced about this point so that the trim was unaffected by a moment from the weight of the model.

In the fixed-trim tests, the load was adjusted by counterweights. The range of trims was selected to include the best trim and the trim for zero trimming moment at all loads and speeds of interest. Static drafts and trimming moments were obtained over the same range of loads for the determination of the water lines at rest and the static stability.

Results and Discussion

The results of the hydrodynamic tests were reduced to the usual coefficients based on Froude's law to make them independent of size. In this case, the beam over the spray strips was chosen as the characteristic dimension. The nondimensional coefficients are defined as follows:

Load coefficient, $C_\Delta = \Delta/wb^3$

Resistance coefficient, $C_R = R/wb^3$

Speed coefficient, $C_V = V/\sqrt{gb}$

Trimming-moment coefficient, $C_M = M/wb^4$

Rise coefficient, $C_r = r/b$

Draft coefficient, $C_d = d/b$

where

Δ   is load on water, pounds.

w,   specific weight of water, pounds per cubic foot
      (63.3 for these tests, usually taken as 64
      for sea water).

b,   beam over spray strips, feet.

R,   resistance, pounds.

V,   speed, feet per second.

g,   acceleration of gravity, 32.2 feet per second
      per second.

M,   trimming moment, pound-feet.

r,   rise of center of gravity (height above its
      position at rest), feet.

d,   draft at main step, feet.

Any consistent system of units may be used. The moment data are referred to the center of moments shown in figure 1. Tail-heavy moments are considered positive. Trim is the angle between the base line of the model and the horizontal.

Free-to-trim tests.- All the free-to-trim tests were made at an initial load coefficient C_{Δ_0} of 1.575 and the hydrofoil lift device was set to reduce the load to zero at a speed coefficient C_V of 10.0. This loading corresponds to surplus buoyancy of approximately 95 percent for the form of deck used in the series.

The results of the tests of model 57-B at four fore-and-aft positions of the center of gravity are shown in figure 3. The distance of the center of gravity above the keel is constant at 24.00 inches. At speed coefficients around 2.2 to 2.5, the resistance curves have an early hump because the bow is deeply immersed at those speeds, and heavy spray and high resistance result. The trims are lower than those for minimum resistance. Moving the center of gravity forward results in a further reduction in trim, a deeper immersion of the bow, and a higher resistance. The true hump speed corresponding to the highest trim and the maximum resistance at best trim occurs near a

speed coefficient of 3.5. At this point, the bow is dry and has no large effect on the resistance. The trim is approximately that for minimum resistance; moving the center of gravity therefore has little effect on resistance at this speed. At high speeds, the position of the center of gravity has a greater effect, but this effect is more readily controlled by use of the elevators.

In all of the other free-to-trim tests, the center of gravity was at the center of moments shown on figure 1 (36.1 percent beam forward of the step).

The free-to-trim characteristics of models 57-A, 57-B, and 57-C are compared in figure 4. At the true hump speed ($C_V = 3.5$), the effect of the angle of dead rise on resistance and trim is almost negligible. At higher speeds, resistance and trim increase with increase in dead rise.

Figure 4 also shows the effect of extending the bow of model 57-B forward 10 inches as shown in figure 1 (model 57-B-5). This modification greatly reduces the resistance in the region of the low-speed hump and results in a cleaner running bow, as shown in figure 5. The test indicates that the original forebody used for the series is too short for the assumed loading. Inasmuch as the low-speed hump in the resistance curves of any of the models can be eliminated by extending the bow, further comparisons in this region are of little value. With an extended bow, the maximum resistance of any of the models will occur at the true hump speed near a speed coefficient of 3.5.

Model 57-A was run both with and without spray strips and the results are given in figures 6, 7, and 8. The spray strips reduce the resistance and the trim at the hump speed and greatly reduce the spray at all speeds. From the spray photographs, it is apparent that some form of chine flare or spray strip is essential for adequate control of spray with the high load coefficients used for floats.

General tests.- The results of the general tests of models 57-A, 57-B, and 57-C are summarized in figures 9 and 10. It should be noted that the low-speed hump in the resistance curves at zero trimming moment can be suppressed either by extending the bow or by increasing the trim to bring the bow clear of the water because this hump does not occur in the curves at best trim. This hump should

therefore be disregarded in the analysis unless the short forebody is of interest for aerodynamic or structural reasons.

At zero trimming moment, the effect of angle of dead rise over a wide range of load is small at the true hump speed; whereas resistance and trim tend to increase with angle of dead rise at planing speeds. At best trim, a comparison of more general interest, the effect of angle of dead rise on resistance is negligible up to the hump speed but becomes marked as soon as this speed is reached. At planing speeds, the trend is similar to that obtained with planing plates (reference 4) in that resistance increases with dead rise. The trim for minimum resistance tends to increase with dead rise, this tendency being more marked at high speeds than at the hump speed. At planing speeds, the corresponding trimming moments at best trim are not greatly affected by the angle of dead rise. The maximum positive trimming moments, however, become larger as the angle of dead rise is decreased.

Photographs of spray at the hump speed (figs. 11 and 12) indicate that, at the same trim, the height of the spray decreases with increase in dead rise. The tendency is consistent over a range of loadings.

The load-resistance ratio Δ/R at the true hump speed $(C_V = 3.50)$ varies approximately linearly from 5.1 at a load coefficient of 0.9 to 4.4 at a load coefficient of 1.8 for all the models. At this speed, the values of Δ/R at zero trimming moment and at best trim are about the same for each model.

Model 57-B was also tested with 5° and 9° angle of afterbody keel and with 0.45 inch and 1.25 inches depth of step. At best trim, the effects of varying these parameters over such wide ranges are generally similar to those reported in references 5 and 6. Increasing the depth of step results in a small increase in resistance at the hump speed and a decrease at high speeds and light loads. Increasing the angle of afterbody keel has the same effect as increasing the depth of the step but the effect is more marked at the hump speed and less marked at high speeds. At zero trimming moment, 5° angle of afterbody keel results in a very high low-speed hump in the resistance curve, when the forebody is short as in model 57-B, because the trim is lower and the bow is more deeply immersed than with 7° angle of keel.

Static properties.- The static properties of the mod-
els at the initial load coefficient used in the free-to-
trim tests are compared in figure 13. The trim at rest
decreases slightly with increase in dead rise, and the
draft increases. The extended bow increases the trim at
rest and, of course, adds considerably to the positive
trimming moment at negative trims.

Design charts.- Charts for the determination of the
resistance and the trimming moment of models 57-B and 57-B-5
are given in figures 14 and 15, respectively. The use of
these charts in design problems concerned with the water
resistance at arbitrary trims or trimming moments is de-
scribed in reference 7. For twin-float seaplanes at the
usual spacing between floats required for lateral stabil-
ity at rest, the forces acting on the float system may be
assumed to be twice those for one float (reference 8).

The static properties of models 57-B and 57-B-5 are
given in figures 16 and 17, respectively. These charts
are useful for determining the water line at rest and the
longitudinal righting moments for various initial load
coefficients and positions of the center of gravity.

In figures 14 to 17, the trimming-moment coefficients
are referred to the center of moments shown in figure 1.

AERODYNAMIC TESTS

Test Procedure

The aerodynamic tests of the models were made in the
N.A.C.A. 7- by 10-foot wind tunnel (reference 9). The air
drag was measured at a dynamic pressure of 16.37 pounds
per square foot, corresponding to an air speed of about 80
miles per hour at standard sea-level atmospheric condi-
tions. The range of pitch angles was from -10° to 16°,
measured at 2° intervals from the base line.

The models were mounted inverted on the standard
single-spindle support in the center of the air stream.
Inasmuch as a small part of the spindle was exposed to the
air, tests were also made with a dummy support in place to
obtain the tare drag. Figure 18 shows model 57-B mounted
in the tunnel.

Results and Discussion

The data were reduced to coefficient form by means of the relation $C_D = \dfrac{D}{q \, (vol)^{2/3}}$

where C_D is the drag coefficient.

   D,   drag of float.

   q,   dynamic pressure $(1/2 \, \rho \, V^2)$.

   vol,   volume of float.

The drag coefficient is based on volume rather than area because the volume of a float is an independent design variable.

The data are presented in figure 19 as curves of C_D plotted against pitch angle. The pitch angle is referred to the base line in figure 19(a) and to the angle for minimum drag in figure 19(b).

Model 57-A has the smallest angle of dead rise and likewise the lowest values of C_D; model 57-C with the largest angle of dead rise has the highest values of C_D.

The large increase in drag caused by spray strips is shown by the C_D curves of model 57-A with and without spray strips. The strips are approximately 4 percent of the maximum beam and increase the drag about 10 to 15 percent in the flying range.

CONCLUSIONS

1.   The effect of angle of dead rise on water resistance in the range from 20° to 30° was negligible up to and including the hump speed. At planing speeds, the resistance increased with an increase in the angle of dead rise, a trend similar to that obtained with planing plates.

2.   The height and the amount of spray at the hump speed tended to decrease with an increase in the angle of dead rise from 20° to 30°.

3. The aerodynamic drag increased slightly with an increase in the angle of dead rise from 20° to 30°.

4. For floats having the usual cross-sectional shape and load coefficients for minimum allowable surplus buoyancy, the length-beam ratio of the forebody should be approximately 4.0, or larger, to run cleanly at low speeds on the water. Too short and bluff a forebody will result in excessive spray and resistance at speeds below the hump speed.

5. Spray strips were an effective means of reducing spray at the high loadings employed with seaplane floats, but they caused high aerodynamic drag.

Langley Memorial Aeronautical Laboratory,
    National Advisory Committee for Aeronautics,
        Langley Field, Va., June 6, 1939.

REFERENCES

1. Parkinson, J. B.: Tank Tests of Models of Floats for
        Single-Float Seaplanes - First Series. T.N. No.
        563, N.A.C.A., 1936, fig. 1.

2. Truscott, Starr: The N.A.C.A. Tank - A High-Speed
        Towing Basin for Testing Models of Seaplane Floats.
        T.R. No. 470, N.A.C.A., 1933.

3. Allison, John M.: Tank Tests of a Model of the Hull
        of the Navy PB-1 Flying Boat - N.A.C.A. Model 52.
        T.N. No. 576, N.A.C.A., 1936.

4. Shoemaker, James M.: Tank Tests of Flat and V-Bottom
        Planing Surfaces. T.N. No. 509, N.A.C.A., 1934.

5. Allison, John M.: The Effect of the Angle of After-
        Body Keel on the Water Performance of a Flying-
        Boat Hull Model. T.N. No. 541, N.A.C.A., 1935.

6. Bell, Joe W.: The Effect of Depth of Step on the
        Water Performance of a Flying-Boat Hull Model -
        N.A.C.A. Model 11-C. T.N. No. 535, N.A.C.A., 1935.

7. Dawson, John R.: A General Tank Test of a Model of the
        Hull of the P3M-1 Flying Boat Including a Special
        Working Chart for the Determination of Hull Per-
        formance. T.N. No. 681, N.A.C.A., 1938.

8. Herrmann, H., Kempf, G., and Kloess, H.: Tank Tests
        of Twin Seaplane Floats. T.M. No. 486, N.A.C.A.,
        1928, p. 13.

9. Wenzinger, Carl J., and Harris, Thomas A.: Wind-
        Tunnel Investigation of an N.A.C.A. 23012 Airfoil
        with Various Arrangements of Slotted Flaps. T.R.
        No. 664, N.A.C.A., 1939.

TABLE 1

OFFSETS FOR N.A.C.A. MODEL 57-A (INCHES)

Station	Distance from F.P.	Distance from base line							Half-breadth						Deck radius
		Keel	B1 1.20[a]	B2 2.40	B3 3.60	B4 4.80	Chine	Deck	Chine	WL1 9.59[b]	WL2 8.09	WL3 6.59	WL4 5.09	WL5 3.59	
F.P.	0	2.71					2.71	2.71	Tangent at 0.60						
1/4	1.05	5.93	4.30	3.63			3.45	1.36	3.20				0.49	2.50	3.50
1/2	2.10	7.21	5.53	4.61	4.17		4.11	0.97	4.08			0.38	1.68		4.22
1	4.20	8.75	7.23	6.18	5.56	5.29	5.28	0.51	5.02		0.48	1.87			5.03
1½	6.30	9.66	8.40	7.39	6.70	6.33	6.26	0.24	5.53	0.06	1.53	3.88			
2	8.40	10.28	9.20	8.25	7.55	7.14	7.03	0.09	5.79	0.75	2.64				
3	12.60	10.92	10.09	9.34	8.70	8.22	8.04	0	5.97	1.98	5.38				
4	16.80	11.08	10.46	9.88	9.34	8.88	8.58		6.00	3.02					
5	21.00	11.09	10.60	10.13	9.67	9.22	8.84			3.78					
6	25.20		←straight line→				8.91								
7	29.40		←			→	8.91		6.00						
8	33.60		←			→	8.92		5.97						
9	37.80		←			→	8.96		5.86						
10,F	42.00	11.09	←			→	9.02		5.70						
10,A		10.24	←			→	8.17								
11	46.20	9.72	←			→	7.72		5.49						
12	50.40	9.21	←			→	7.30		5.24						
13	54.60	8.69	←			→	6.90		4.93						
14	58.80	8.18	←			→	6.51		4.57						
15	63.00	7.66	←			→	6.14		4.18						
16	67.20	7.14	←			→	5.77		3.77						
17	71.40	6.63	←			→	5.41		3.35						
18	75.60	6.11	←			→	5.05		2.92						
19	79.80	5.60	←			→	4.70		2.47						
A.P.	84.00	5.08	←			→	4.35	0	2.00						

[a] Distance from center line to buttock (B); [b] Distance from base line to water line (WL).

TABLE II

OFFSETS FOR N.A.C.A. MODEL 57-B (INCHES)

Station	Distance from F.P.	Distance from base line							Half - breadth						Deck radius
		Keel	B1 1.20[a]	B2 2.40	B3 3.60	B4 4.80	Chine	Deck	Chine	WL1 9.90[b]	WL2 8.40	WL3 6.90	WL4 5.40	WL5 3.90	
F.P.	0	2.40					2.40	2.40	Tangent at 0.60						
1/4	1.05	5.83	4.06	3.33			3.14	1.20	3.20				0.20	1.38	3.61
1/2	2.10	7.17	5.34	4.35	3.87		3.80	0.86	4.08			0.14	1.16	3.45	4.30
1	4.20	8.51	7.14	5.98	5.29	5.90	4.98	0.45	5.02		0.26	1.41	3.35		5.05
1½	6.30	9.79	8.36	7.23	6.44	6.03	5.95	0.21	5.53		1.16	2.85			
2	8.40	10.47	9.22	8.12	7.33	6.84	6.72	0.08	5.79	0.54	2.07	4.62			
3	12.60	11.19	10.20	9.29	8.52	7.95	7.73	0	5.97	1.58	3.82				
4	16.80	11.39	10.62	9.89	9.22	8.64	8.27		6.00	2.39	5.47				
5	21.00	11.40	10.78	10.18	9.59	9.02	8.53			2.96					
6	25.20		← straight line →				8.60								
7	29.40		←			→	8.60		6.00						
8	33.60		←			→	8.62		5.97						
9	37.80		←			→	8.67		5.86						
10,F	42.00	11.40	←			→	8.74		5.70						
10,A		10.55	←			→	7.89								
11	46.20	10.03	←			→	7.47		5.49						
12	50.40	9.52	←			→	7.07		5.24						
13	54.60	9.00	←			→	6.70		4.93						
14	58.80	8.49	←			→	6.35		4.57						
15	63.00	7.97	←			→	6.02		4.18						
16	67.20	7.45	←			→	5.70		3.77						
17	71.40	6.94	←			→	5.38		3.35						
18	75.60	6.42	←			→	5.06		2.92						
19	79.80	5.91	←			→	4.75		2.47						
A.P.	84.00	5.39	←			→	4.46	0	2.00						

[a] Distance from center line to buttock (B)   [b] Distance from base line to water line (WL)

TABLE III

OFFSETS FOR N.A.C.A. MODEL 57-C (INCHES)

Station	Distance from F.P.	Keel	B1 1.20[a]	B2 2.40	B3 3.60	B4 4.80	Chine	Deck	Chine	WL1 10.23[b]	WL2 8.73	WL3 7.23	WL4 5.73	WL5 4.23	Deck Radius
F.P.	0	2.07					2.07	2.07	Tangent at 0.60						
1/4	1.05	5.71	3.81	3.02			2.81	1.04	3.20					0.82	3.78
1/2	2.10	7.13	5.35	4.07	3.55		3.47	0.74	4.08				0.78	2.16	4.41
1	4.20	8.87	7.03	5.75	5.00	4.66	4.64	0.39	5.02		0.09	1.05	2.42		5.09
1½	6.30	9.93	8.34	7.98	6.20	5.74	5.65	0.18	5.53		0.88	2.23	4.82		5.53
2	8.40	10.67	9.24	7.99	7.07	6.53	6.39	0.07	5.79	0.37	1.66	3.35			
3	12.60	11.48	10.31	9.24	8.33	7.66	7.40	0	5.97	1.28	3.04				
4	16.80	11.72	10.79	9.90	9.09	8.39	7.94		6.00	1.94	4.20				
5	21.00	11.73	10.97	10.23	9.50	8.80	8.20			2.40	4.93				
6	25.20	↑	← straight line →				8.27								
7	29.40		← →				8.27		6.00						
8	33.60		← →				8.28		5.97						
9	37.80	↓	← →				8.35		5.86						
10,F	42.00	11.73	← →				8.44		5.70						
10,A		10.88	← →				7.59								
11	46.20	10.36	← →				7.19		5.49						
12	50.40	9.85	← →				6.82		5.24						
13	54.60	9.33	← →				6.48		4.93						
14	58.80	8.82	← →				6.18		4.57						
15	63.00	8.30	← →				5.89		4.18						
16	67.20	7.78	← →				5.61		3.77						
17	71.40	7.27	← →				5.33		3.35						
18	75.60	6.75	← →				5.07		2.92						
19	79.80	6.24	← →				4.81		2.47						
A.P.	84.00	5.72	← →				4.56	0	2.00						

[a] Distance from center line to buttock (B)   [b] Distance from base line to water line (WL)

TABLE IV

OFFSETS FOR N.A.C.A. MODEL 57-B-5 (INCHES)

Station	Distance from F.P.	Keel	B1 1.20[a]	B2 2.40	B3 3.60	B4 4.80	Chine	Deck	Chine	Deck radius
bow	-10.00	0.49					0.49	0.49	0	0
a	-8.75	3.80	2.10	1.21			1.11	0	2.70	3.84
b	-7.50	5.06	3.41	2.24	1.72		1.71		3.67	4.79
c	-5.00	6.82	5.30	3.98	3.08		2.83		4.74	5.39
d	-2.50	8.09	6.66	5.42	4.47	3.92	3.88		5.30	5.56
F.P.	0.0									
1/4	1.05	9.35	3.09	6.95	6.02	5.35	5.18		5.70	5.73
1	4.20	10.16	8.98	7.90	7.02	6.37	6.14		5.86	
2	8.40	10.88	9.80	8.83	8.05	7.48	7.10		5.95	
3	12.60	11.27	10.35	9.52	8.80	8.21	7.77		5.98	
4	16.80	11.39	10.64	9.95	9.29	8.73	8.27		6.00	
5 and aft		Same as model 57-B, table II								

[a] Distance from center line to buttock (B)
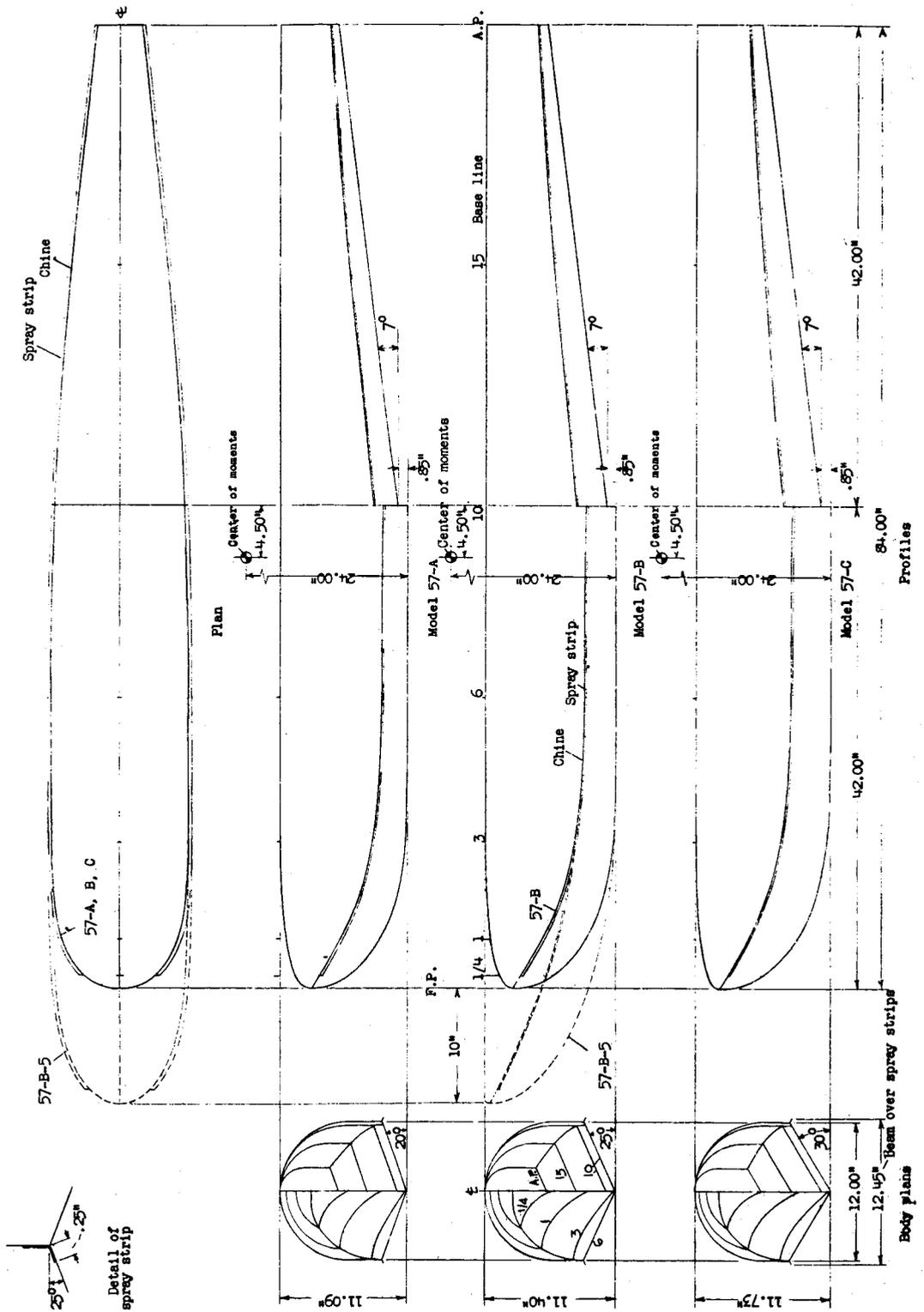
Fig. 1 – Lines of N. A. C. A. model 57 series.

57-A

57-B-5

57-C
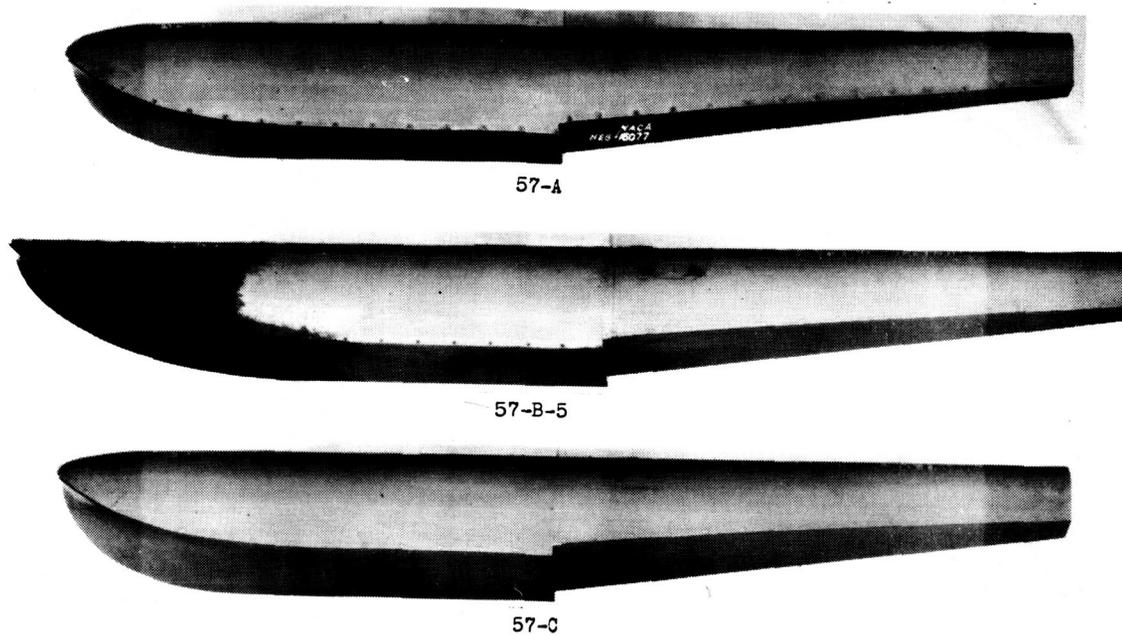
Figure 2.- Photographs of the models. Model 57-B shown with extended bow.
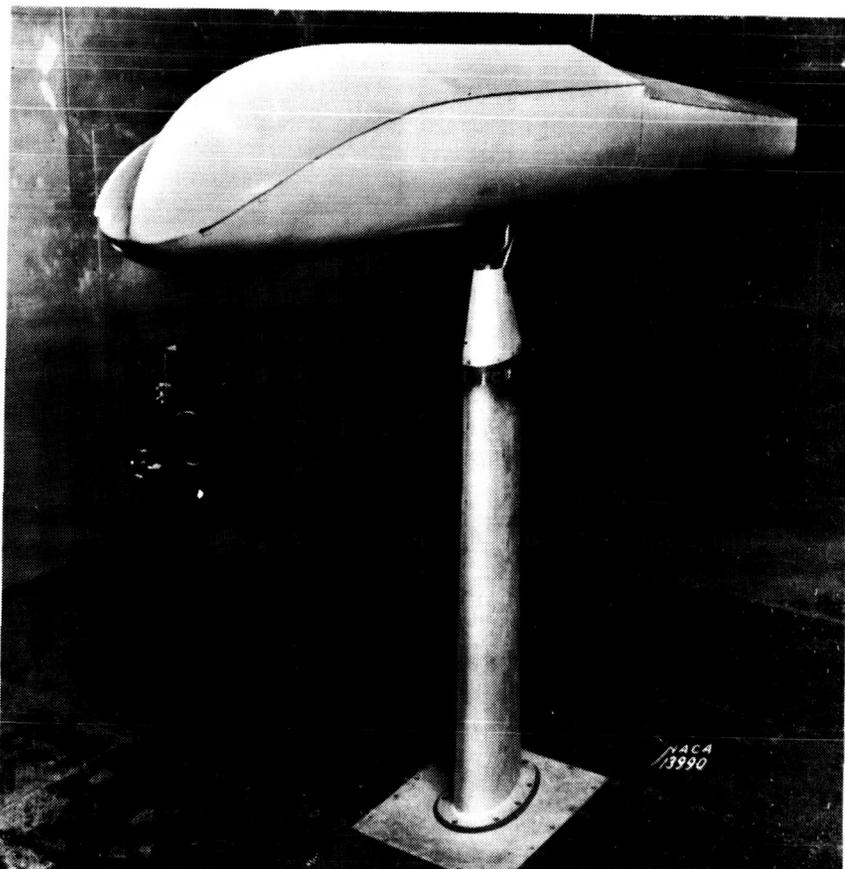
Figure 18.- Model 57-B mounted in the wind tunnel.
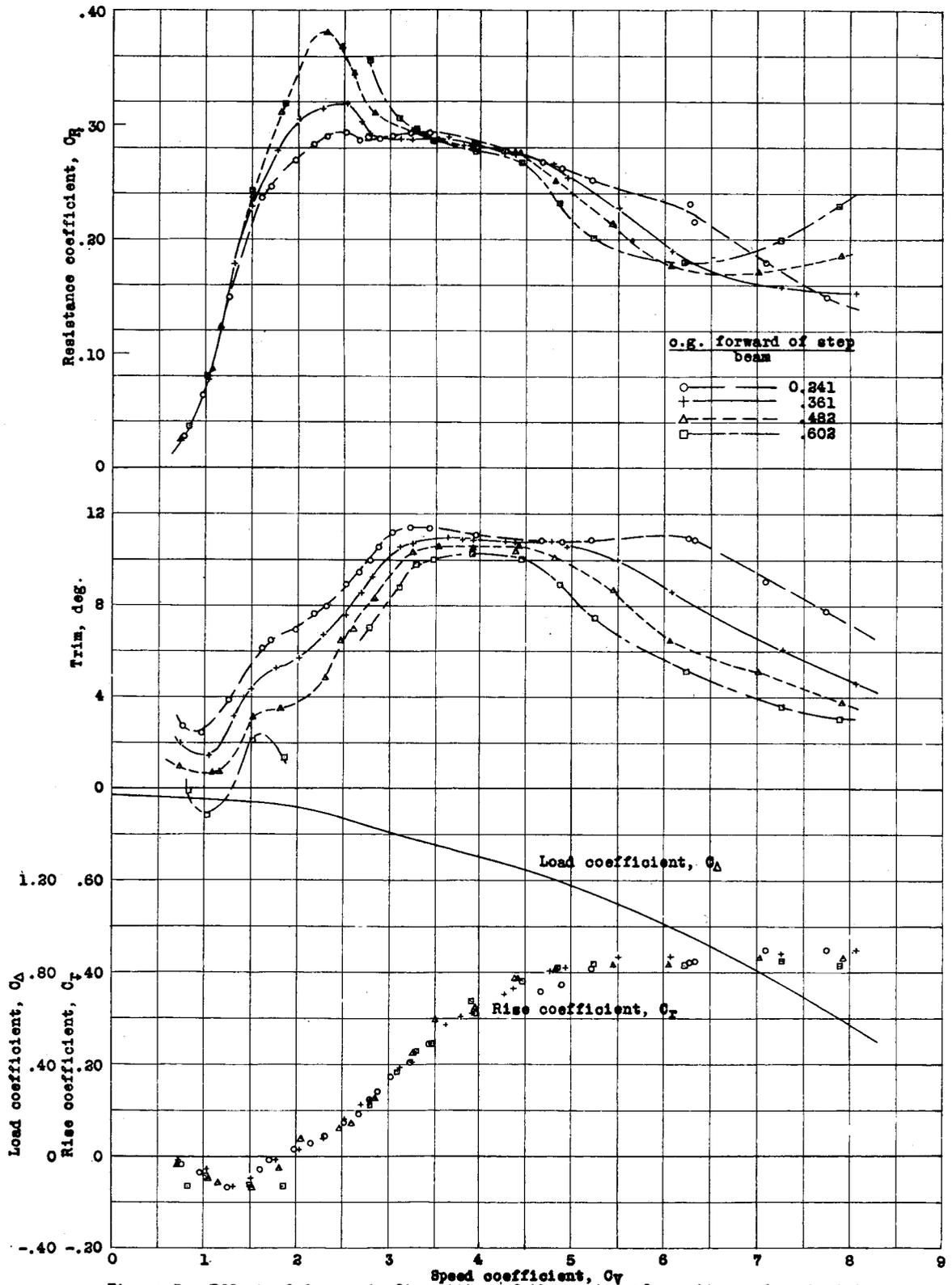
Figure 3.- Effect of fore-and-aft position of the center of gravity on free-to-trim characteristics. Model 57-B.
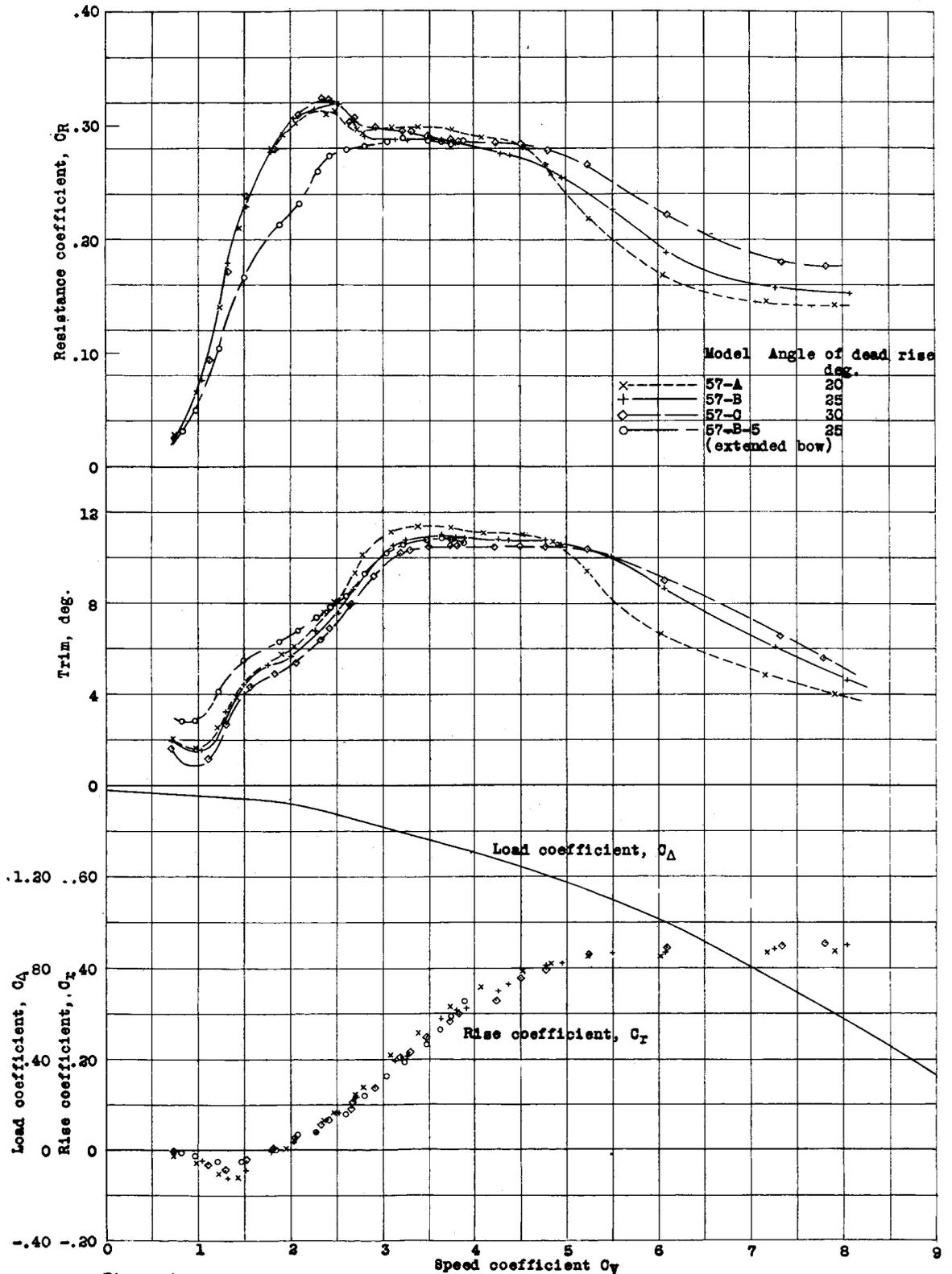
Figure 4.- Effect of angle of dead rise and extended bow on free-to-trim characteristics.

$\tau = 6.6^0$ $\tau = 7.4^0$
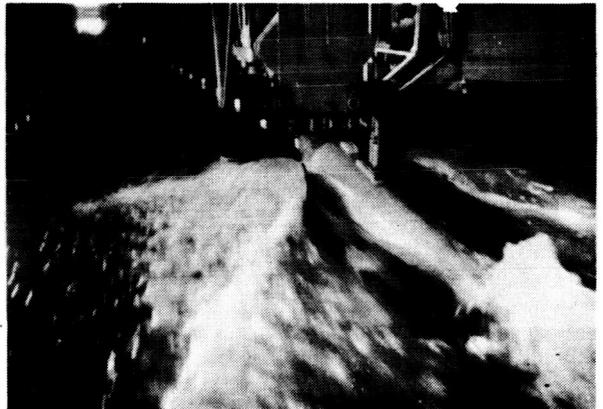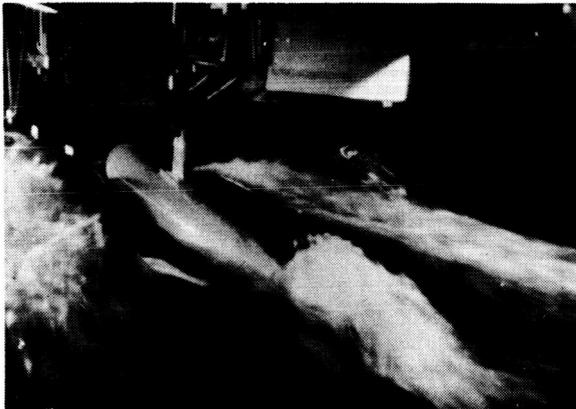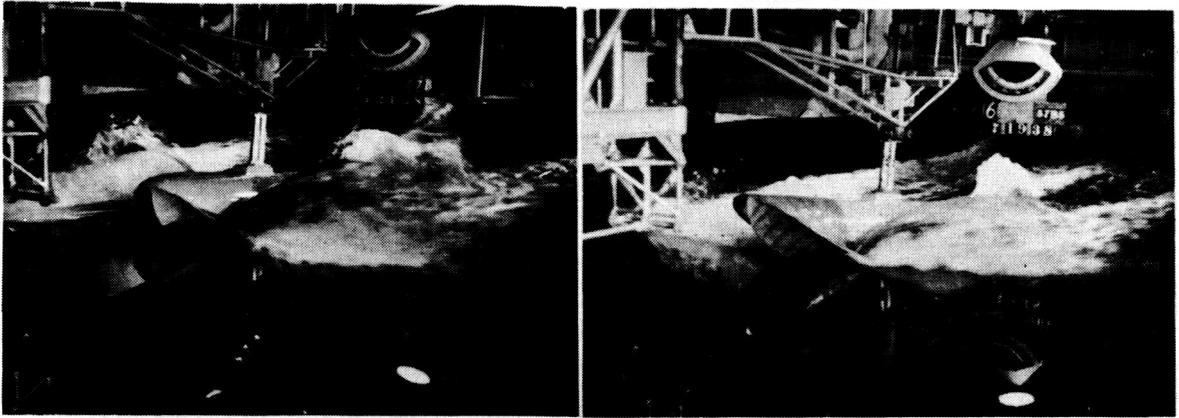
Model 57-B   Model 57-B-5

Short bow   Extended bow

Figure 5.- Effect of extended bow on spray at $C_V = 2.28$ and $C_\Delta = 1.50$. Free to trim.
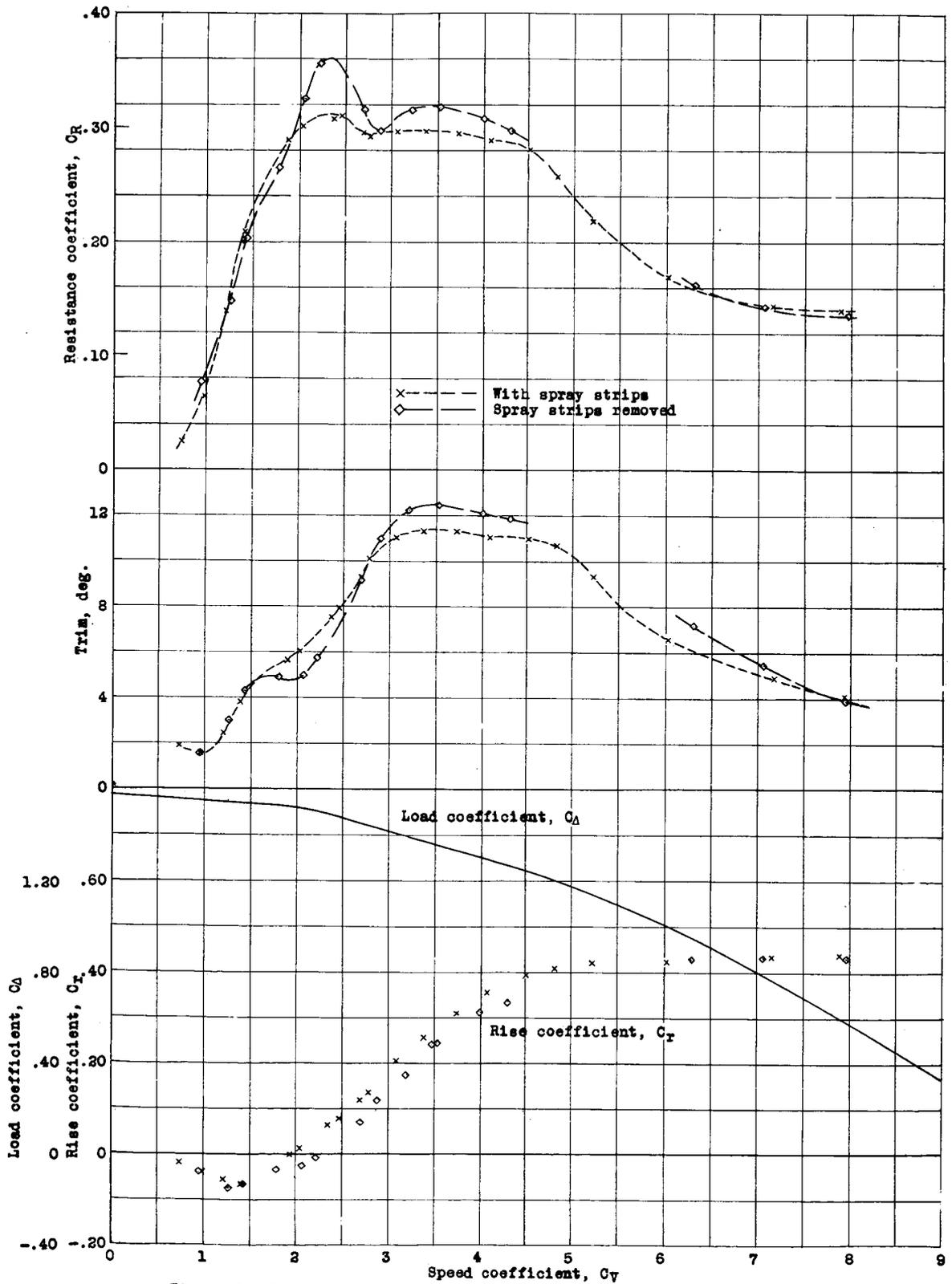
Figure 6.- Effect of spray strips on free-to-trim characteristics. Model 57-A.

$C_V = 1.9,\ C_\Delta = 1.52,\ \tau = 5.6^\circ$ $C_V = 2.2,\ C_\Delta = 1.50,\ \tau = 5.6^\circ$

Model 57-A   Model 57-A-1

With spray strips   Spray strips removed

Figure 7.— Effect of spray strips on spray at low speed. Free to trim.
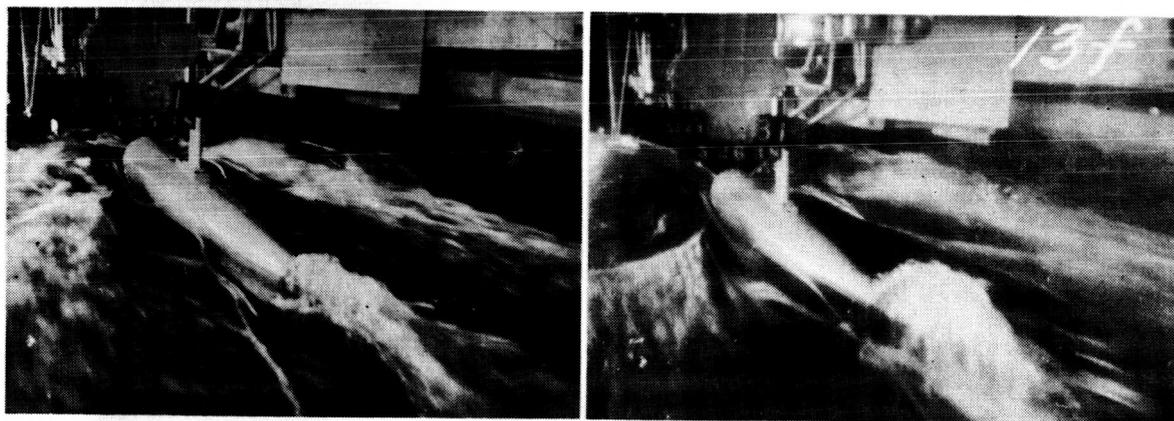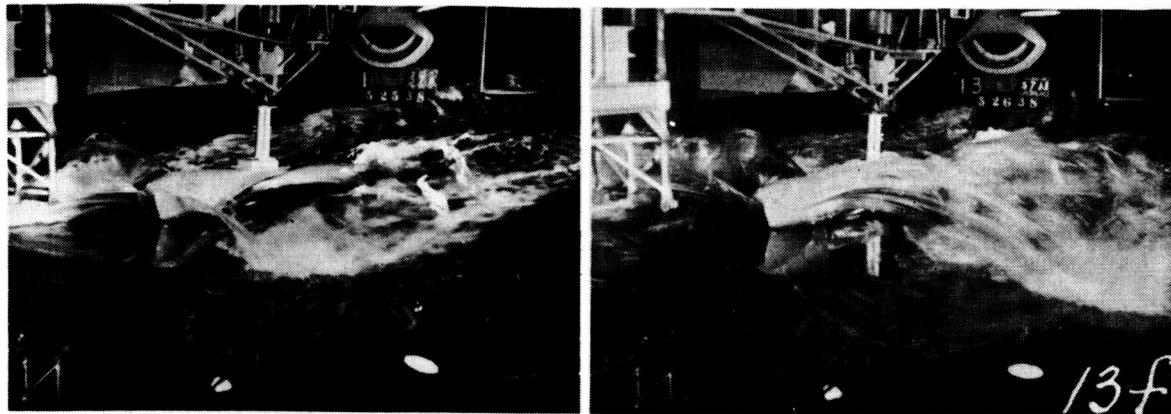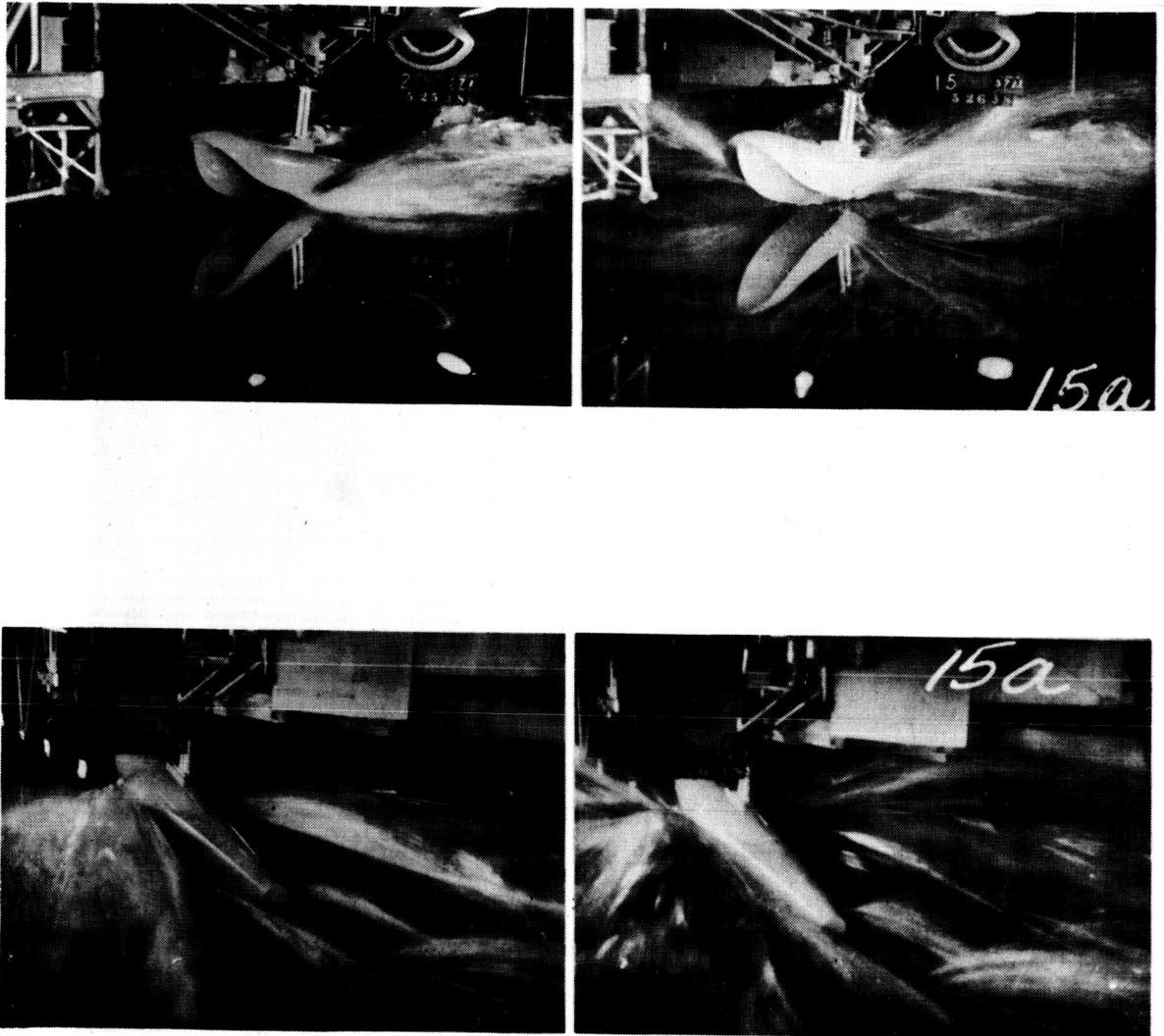
$C_V = 3.4$, $C_\Delta = 1.37$, $\tau = 11.4^\circ$
Model 57-A
With spray strips

$C_V = 3.5$, $C_\Delta = 1.35$, $\tau = 12.5^\circ$
Model 57-A-1
Spray strips removed

Figure 8.- Effect of spray strips on spray at hump speed. Free to trim.
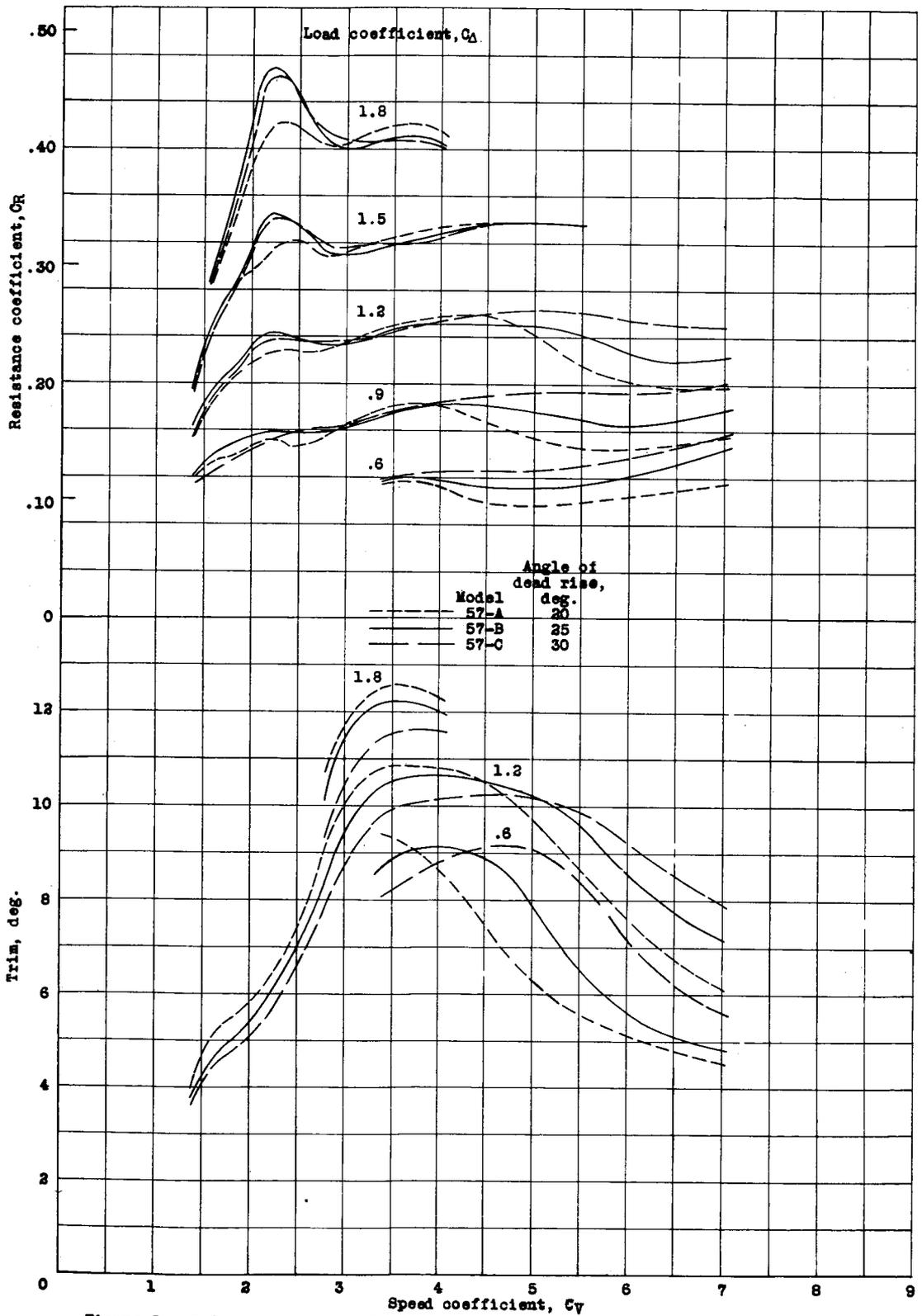
Figure 9.- Effect of angle of dead rise on characteristics at zero trimming moment.

Fig.10
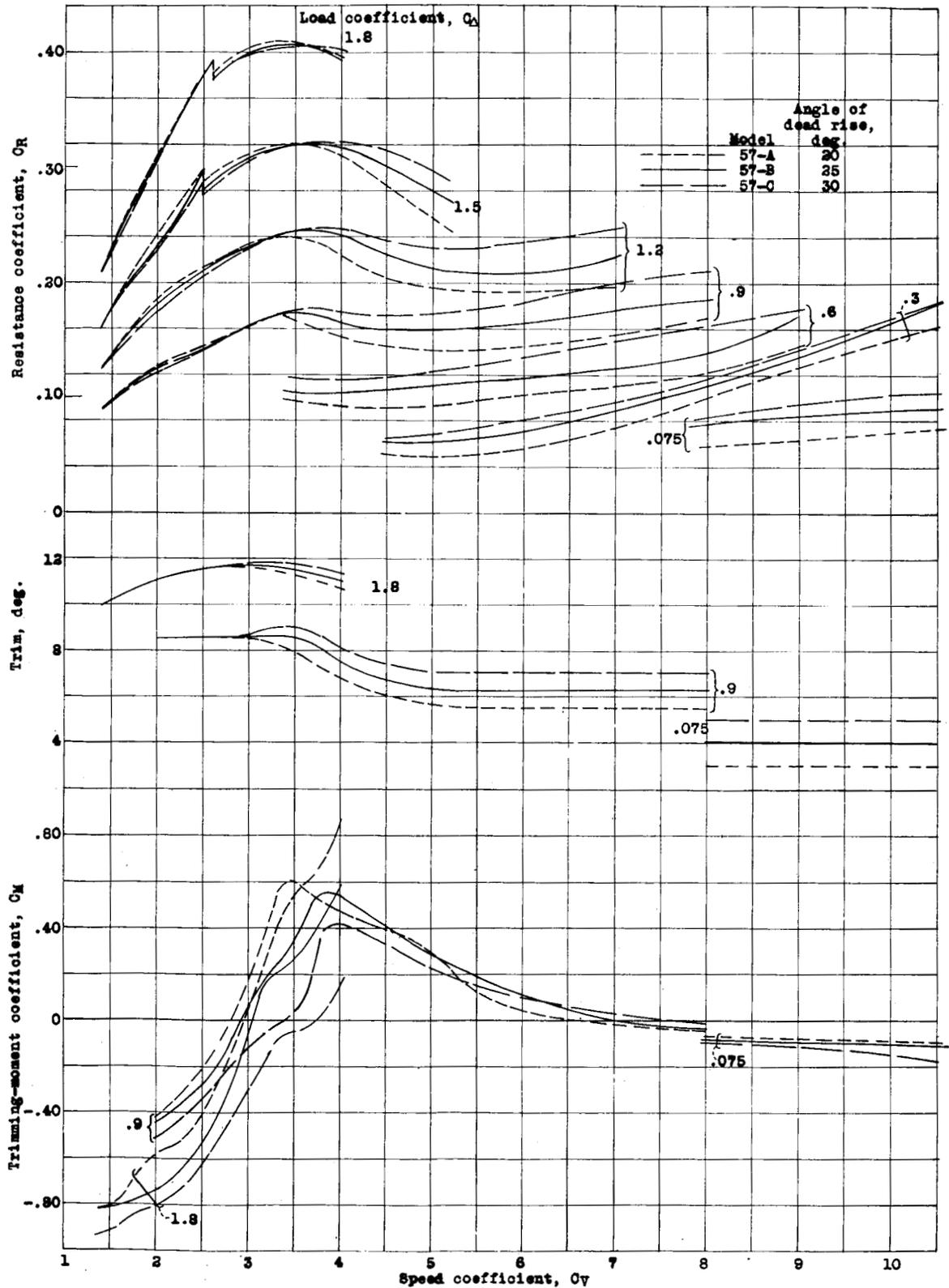
Figure 10.- Effect of angle of dead rise on characteristics at best trim.

$C_\Delta = 1.2$

$C_\Delta = 1.8$
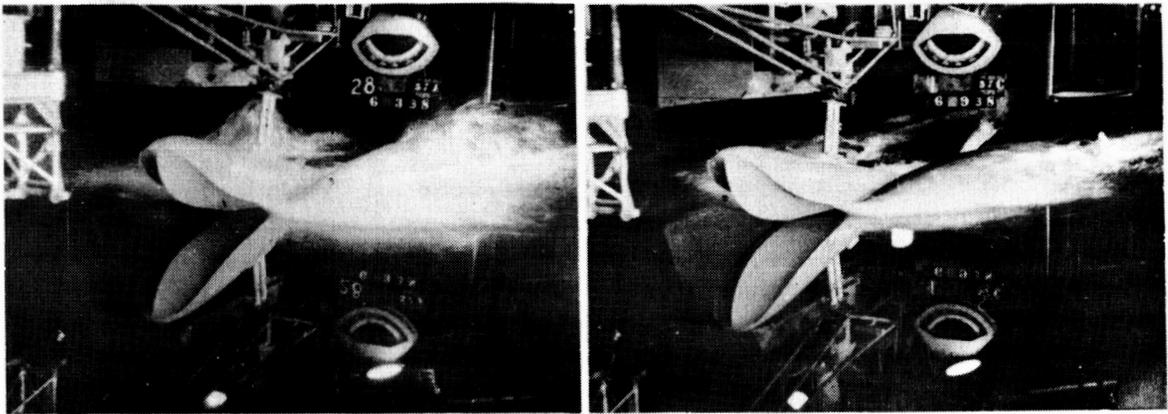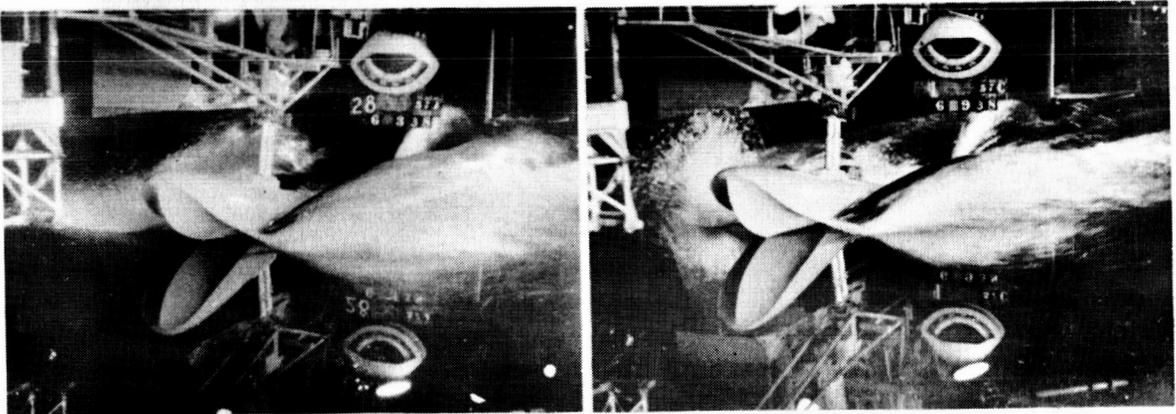
Model 57-A   Model 57-C
Angle of dead rise, 20°   Angle of dead rise, 30°

Figure 11.- Effect of angle of dead rise on spray at hump speed.
C_V , approximately 3.50; 11° fixed trim.

$C_\Delta = 1.2$

$C_\Delta = 1.8$
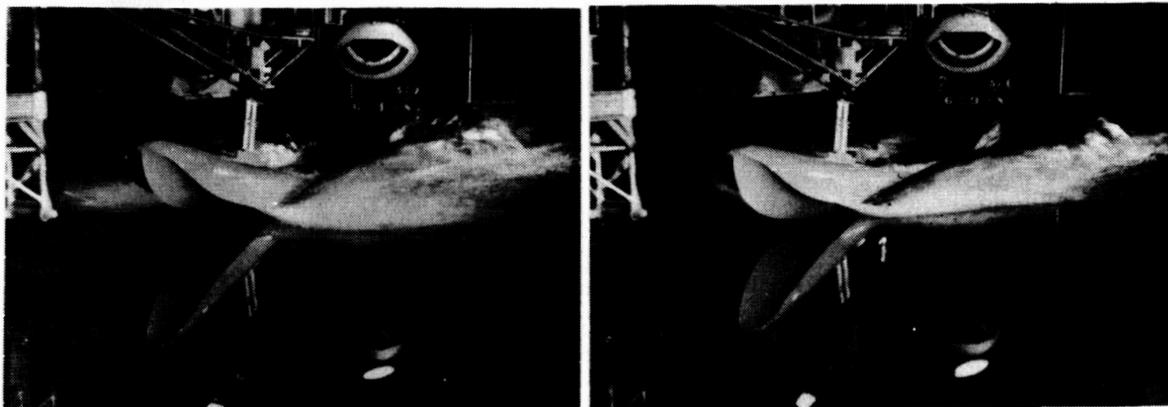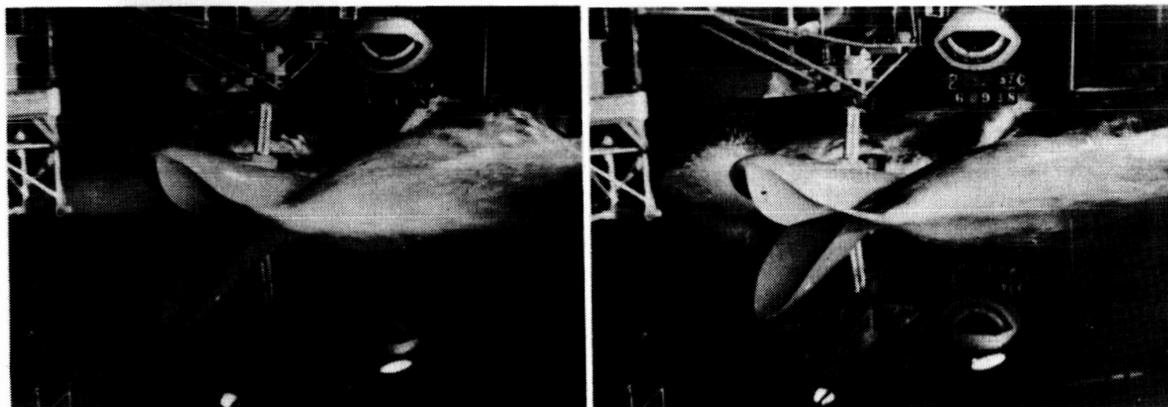
Model 57-A   Model 57-C
Angle of dead rise, 20°   Angle of dead rise, 30°

Figure 12.- Effect of angle of dead rise on spray at hump speed.
C_V ,approximately 3.50; 13° fixed trim.
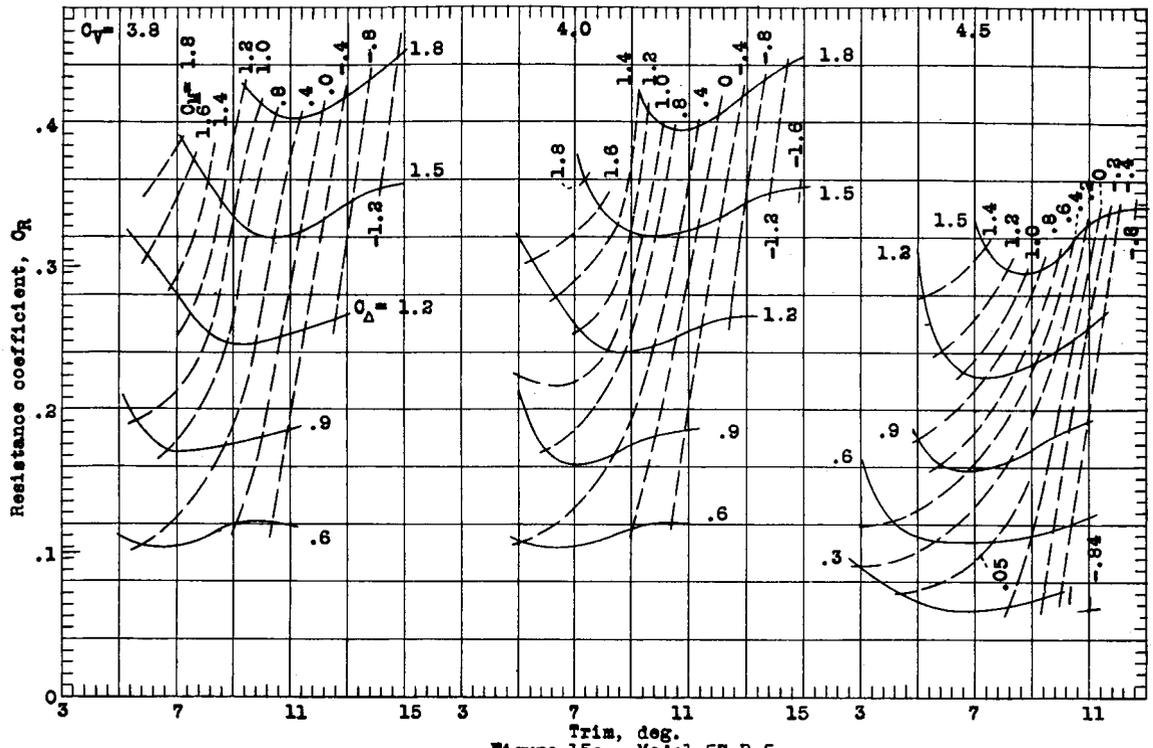
Figure 15c.- Model 57-B-5.
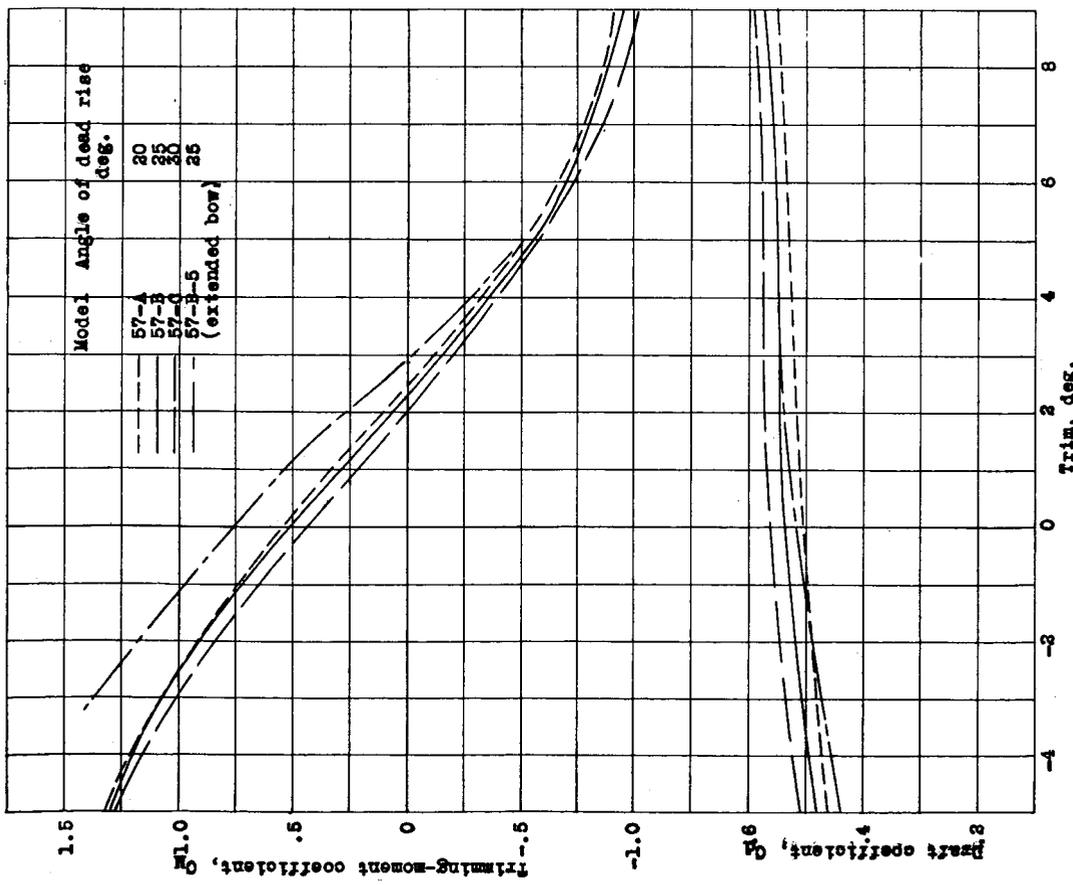
Figure 13.- Effect of angle of dead rise and extended bow on static properties. Initial load coefficient $C_{\Delta_o} = 1.575$.
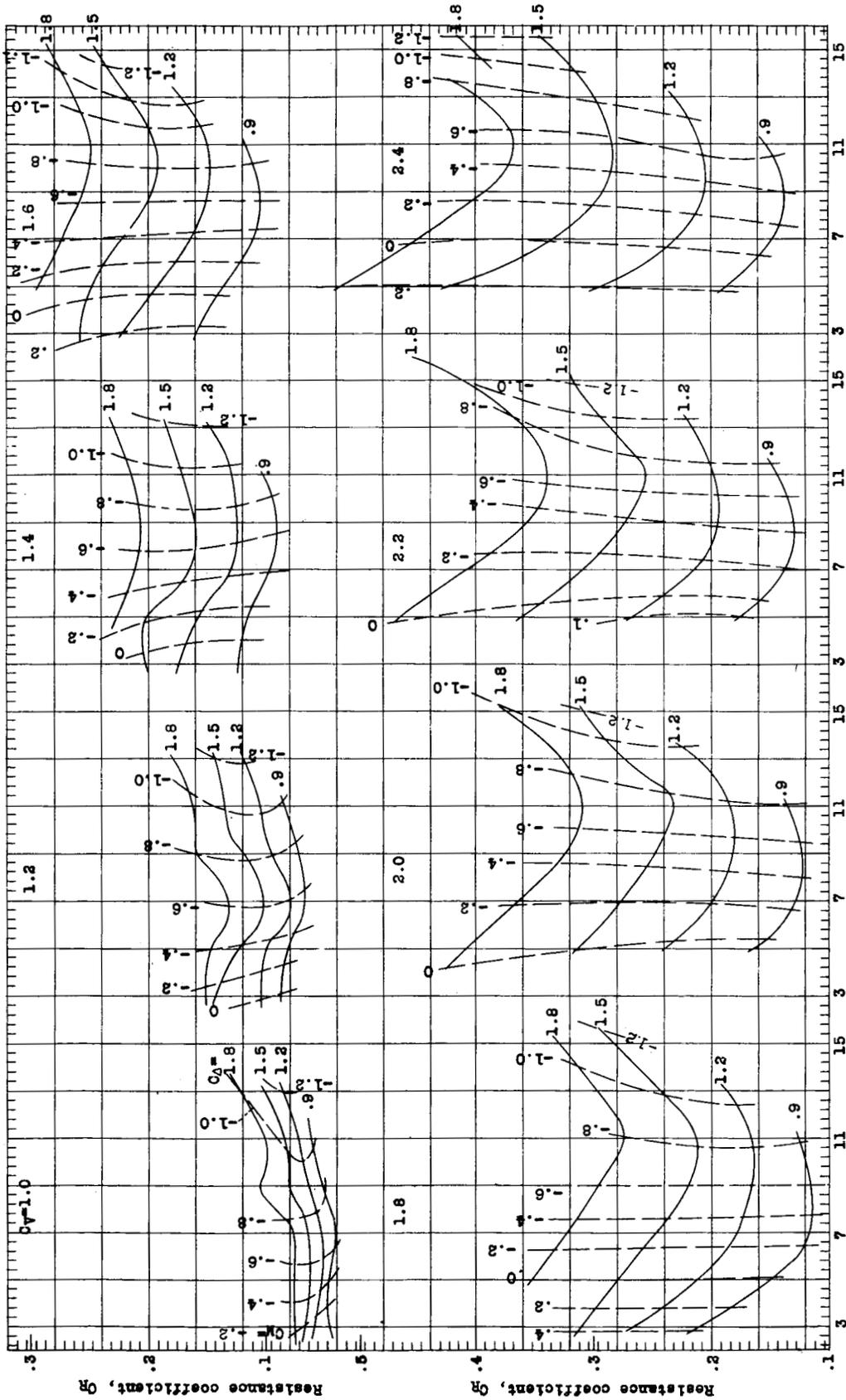
Figure 14a.—Model 57-B. Working charts for the determination of resistance and trimming moment.
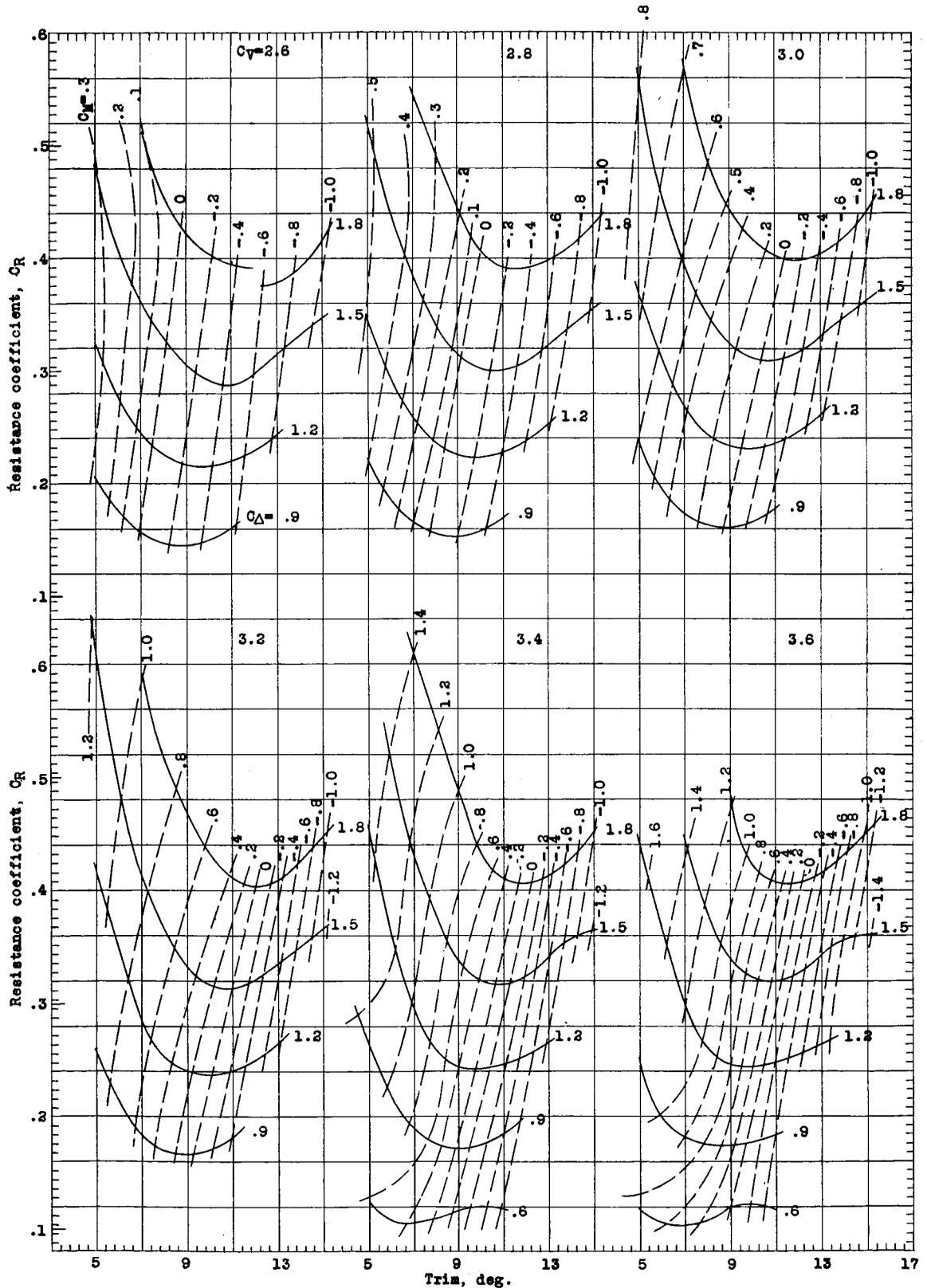
Figure 14b.- Model 57-B.
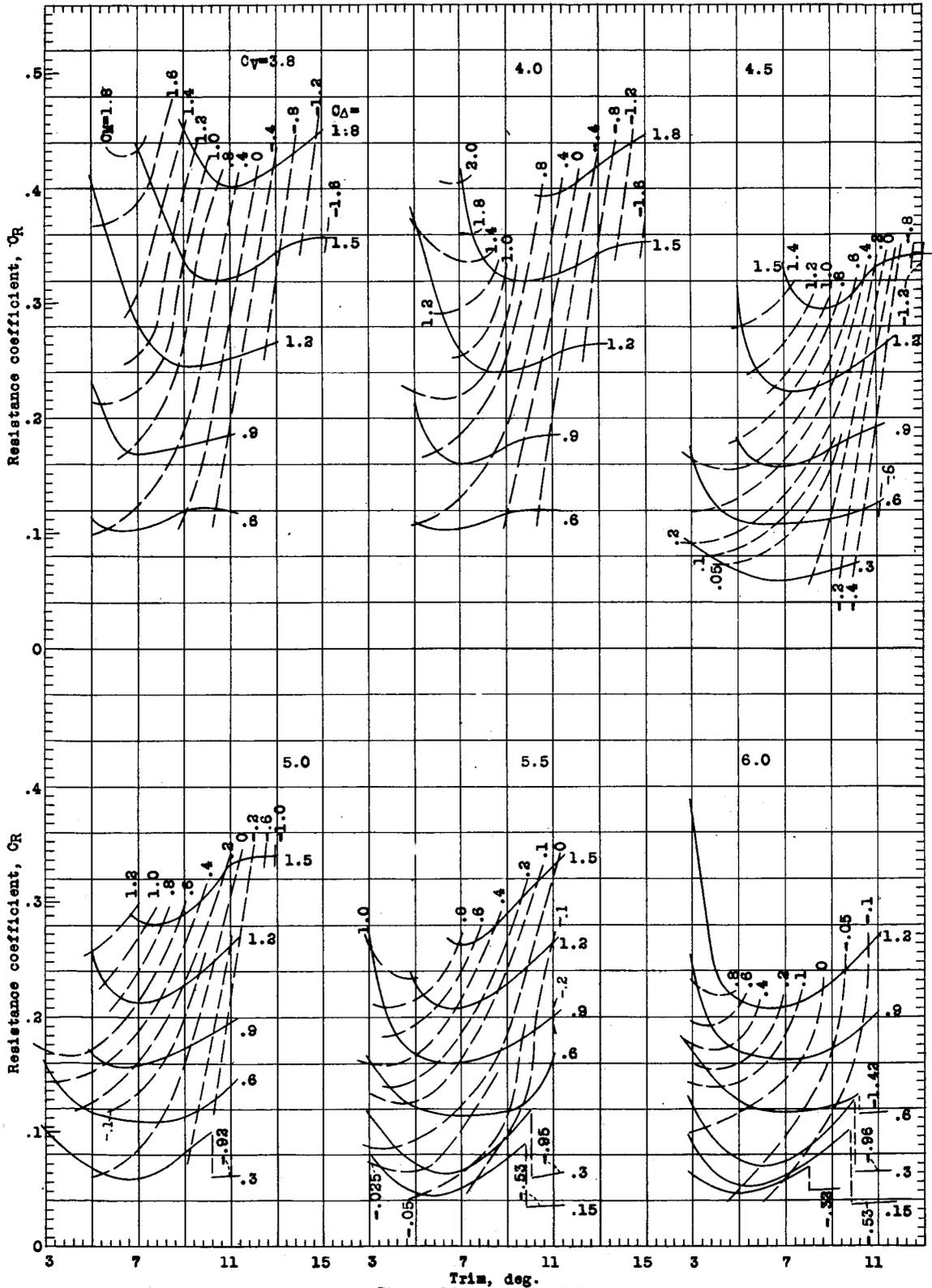
Figure 14c.- Model 57-B.
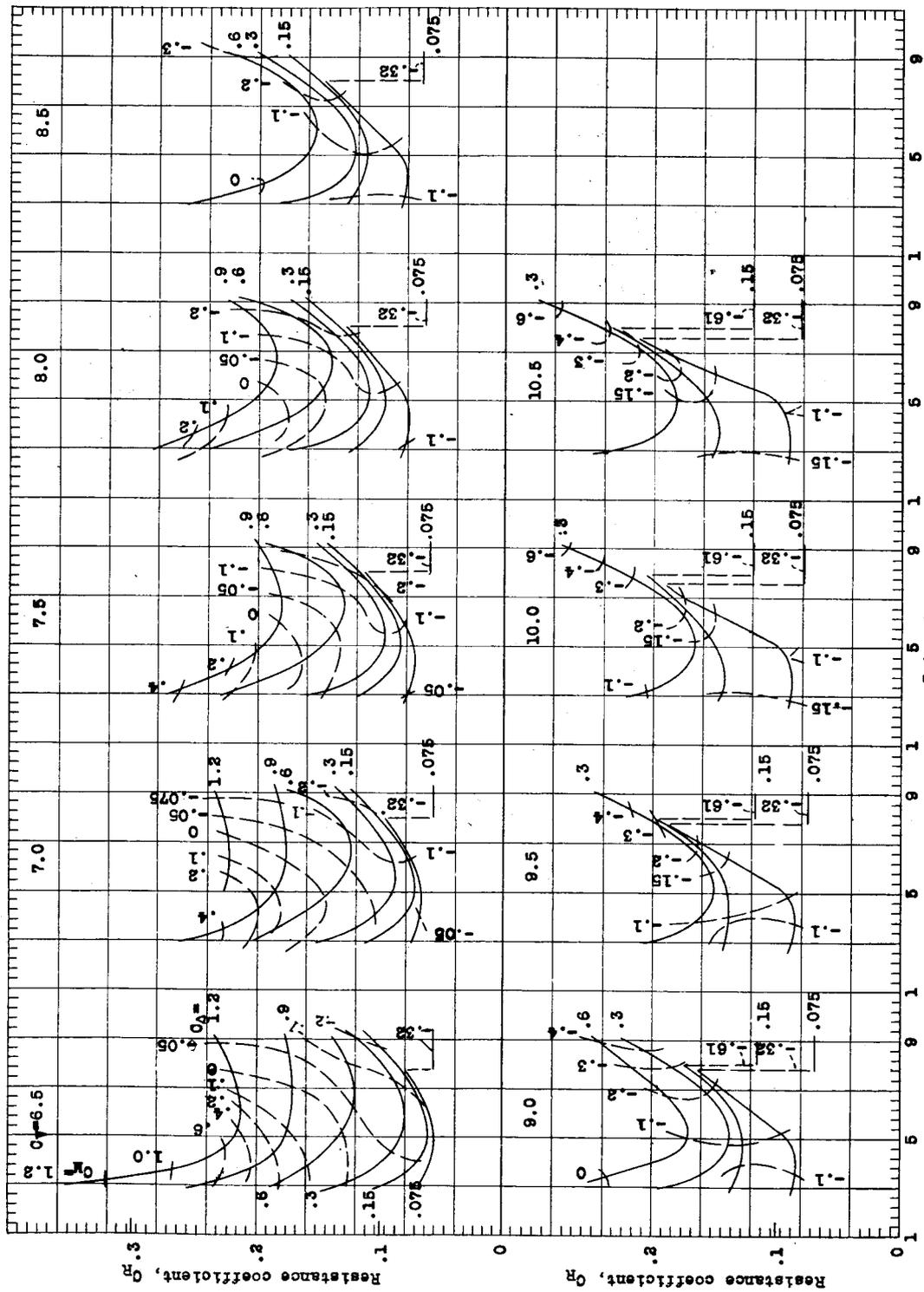
Figure 14d.-- Model 57-B.
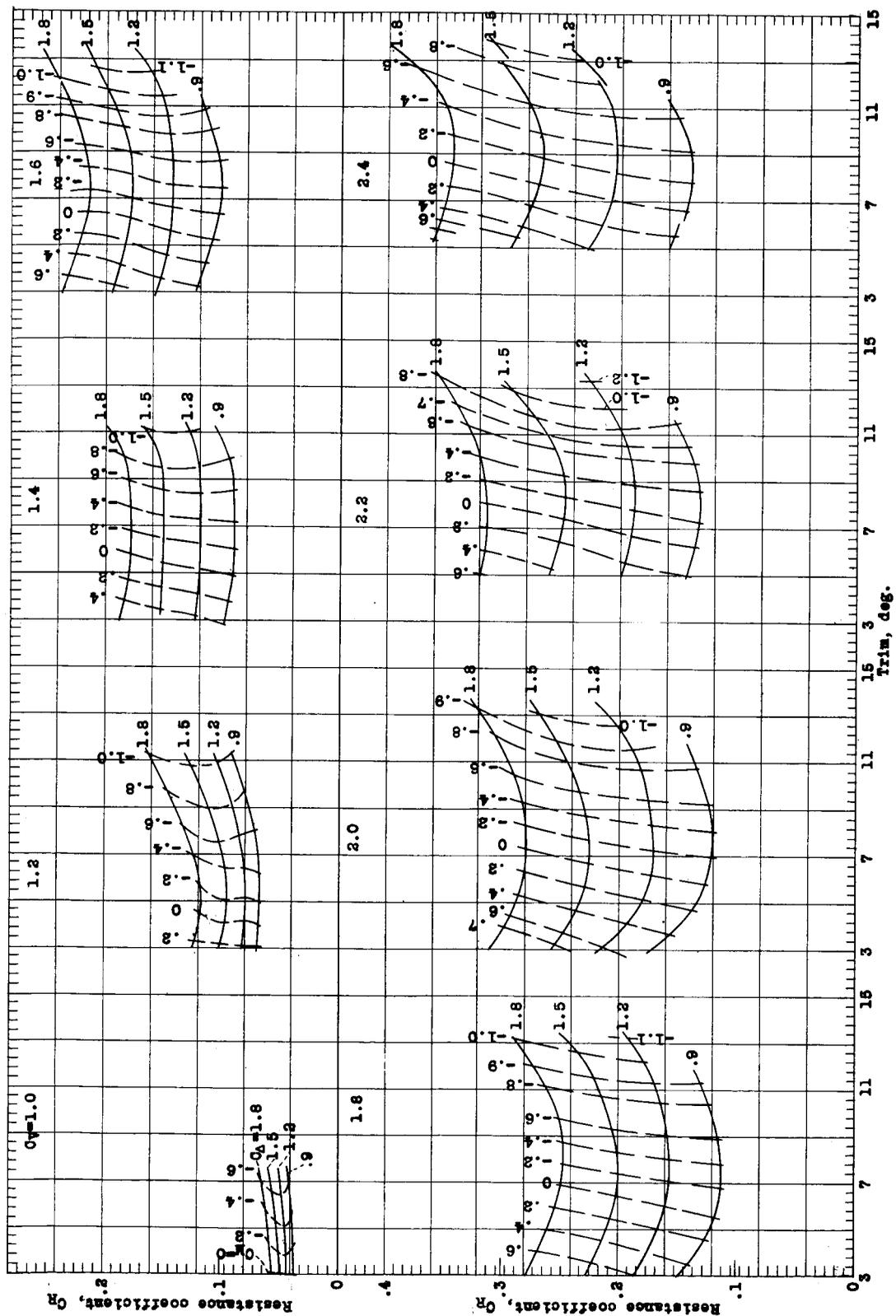
Figure 15a.- Model 57-B-5. Working charts for the determination of resistance and trimming moment.
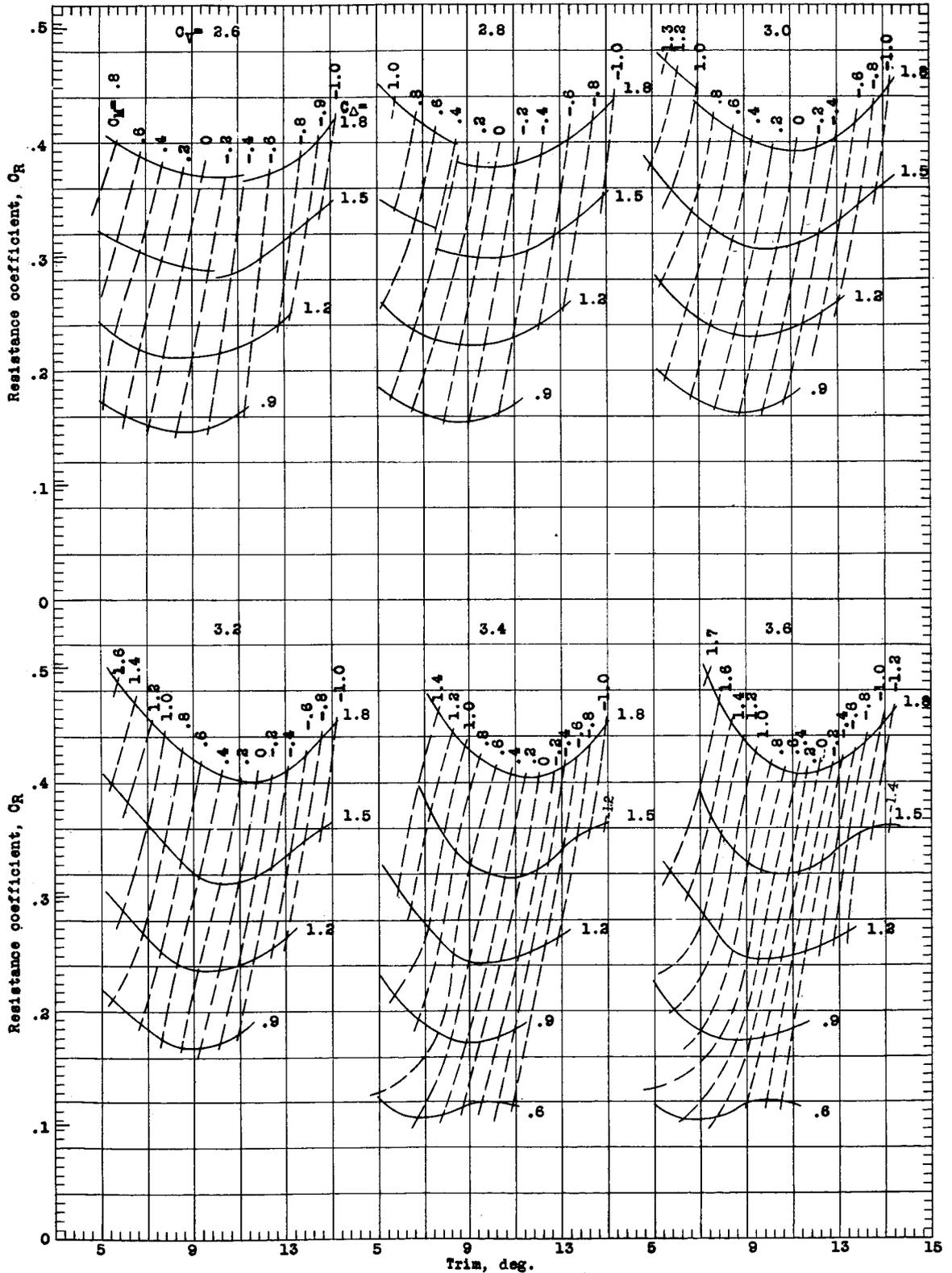
Figure 15b.- Model 57-B-5.
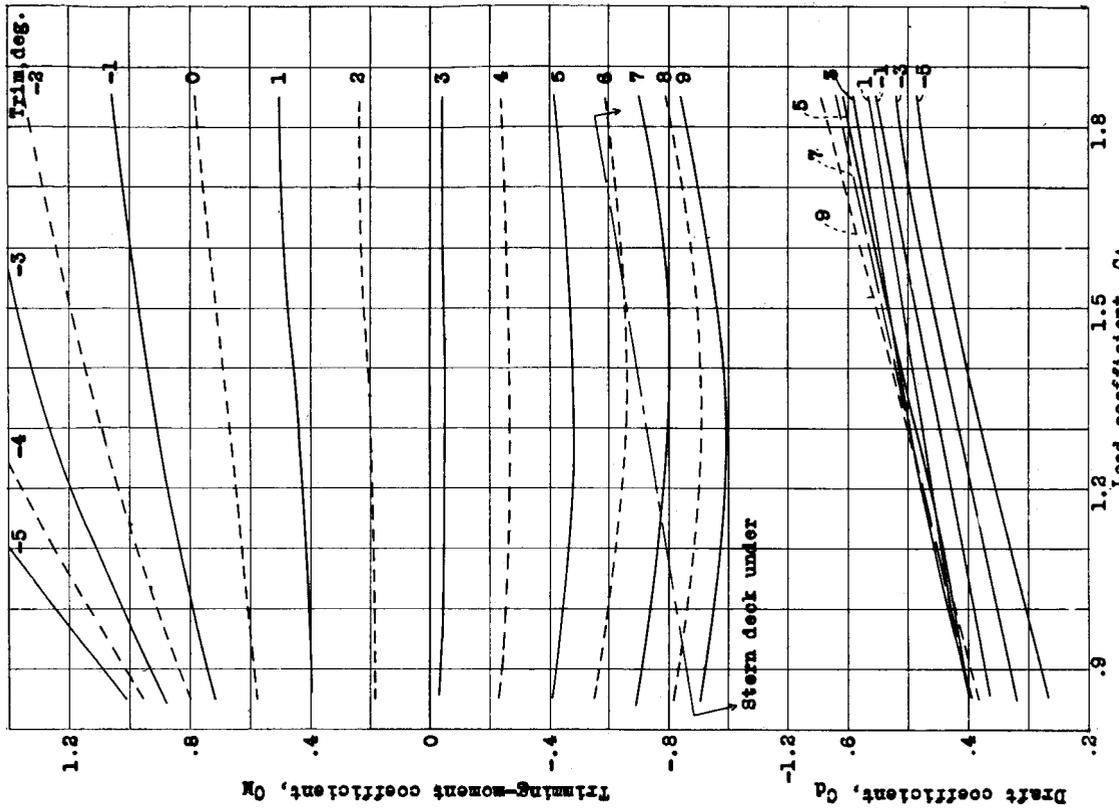
Figure 17.- Model 57-B-5. Static properties.
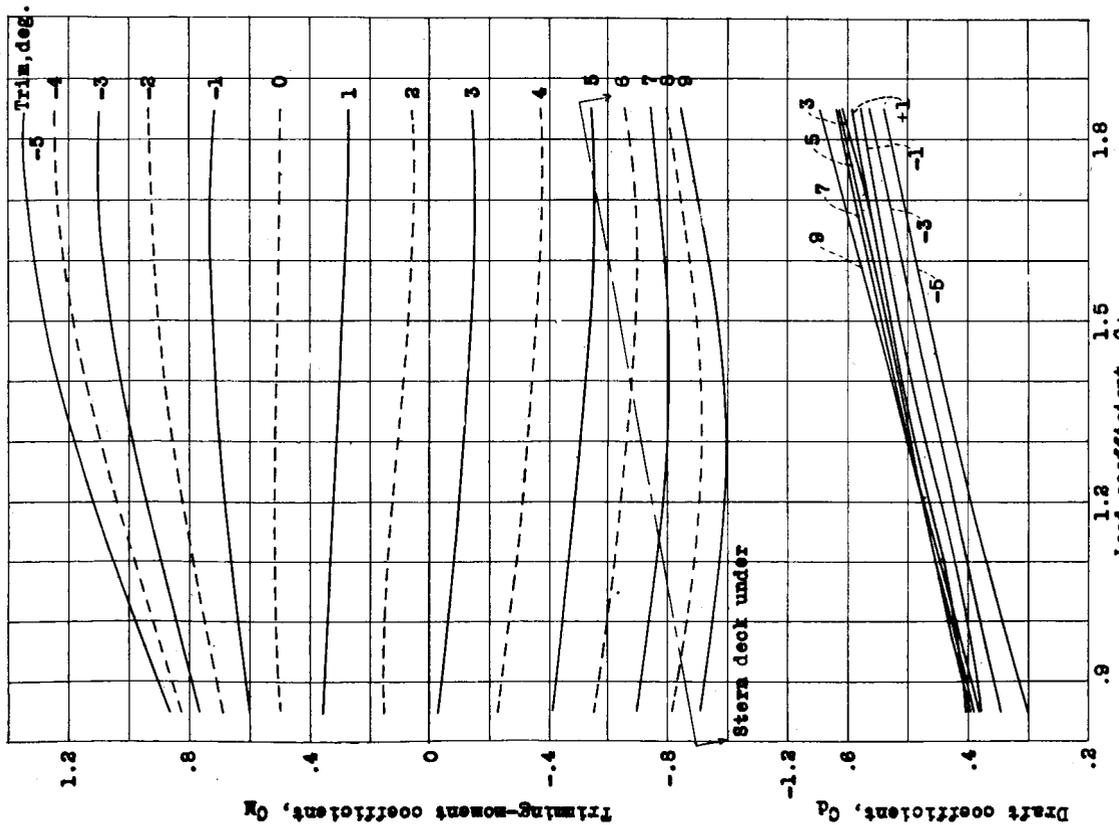
Figure 16.- Model 57-B. Static properties.
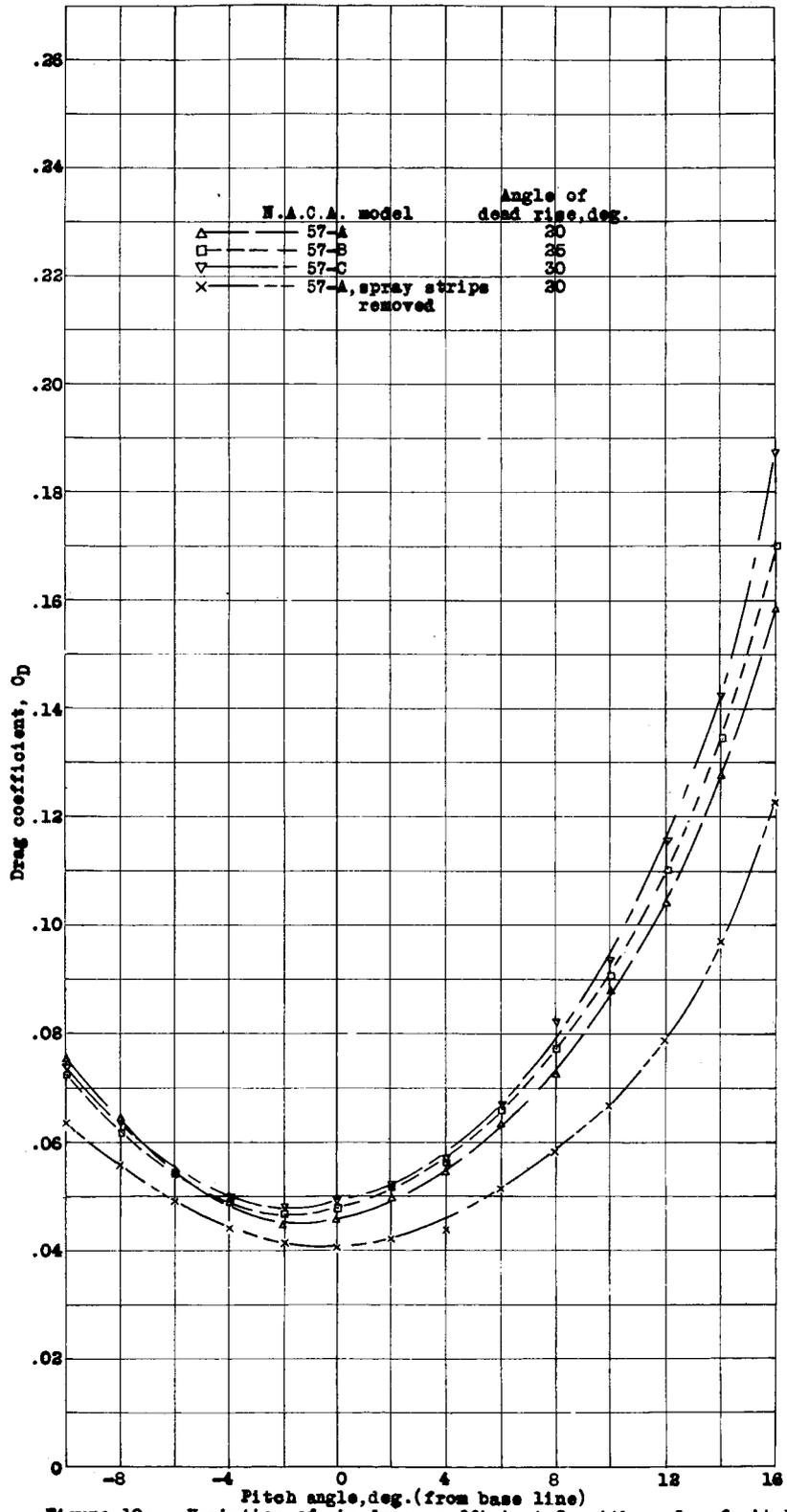
Figure 19a.- Variation of air drag coefficient C_D with angle of pitch.

Figure 19b.